

## Universality class of the conserved Manna model in one dimension

Sang Bub Lee

*Department of Physics, Kyungpook National University, Daegu 702-701, Korea*

(Received 7 March 2014; published 25 June 2014)

The nonequilibrium absorbing phase transition of the discrete conserved Manna model was studied via Monte Carlo simulations on a one-dimensional chain, using the natural initial states with a sequential update. The critical density of the particles was found to be smaller than the recently reported value, and the order-parameter exponent was considerably different from the directed percolation (DP) value. The influence of quenched disorder was also studied on a diluted strip of  $L_x \times L_y$  lattice sites with  $L_x \gg L_y$ , and the results were compared with those of the contact process (CP). It was found that the Manna model and the CP exhibited distinctly different behaviors; the CP exhibited nonuniversal power-law decreases of active-site densities in the Griffith phase, whereas the Manna model showed a standard critical behavior. These results consistently suggest that the Manna model belongs to a universality class that is different from the DP class.

DOI: [10.1103/PhysRevE.89.060101](https://doi.org/10.1103/PhysRevE.89.060101)

PACS number(s): 05.70.Ln, 05.50.+q, 64.60.av, 64.60.De

Universality classes of nonequilibrium absorbing phase transitions (APTs) can be classified by various features of models, such as unconventional symmetries, types of hopping mechanisms of particles, quenched randomness, and conservation laws [1]. Directed percolation (DP) is the most robust class, and various models that yield a continuous phase transition from a fluctuating phase into a single or many absorbing states in a homogeneous one-component system with short-range interactions are known to fall into this class [2,3]. The parity-conserving class and the Manna (conserved-DP) class are also well-established classes classified by, respectively, the symmetry of the absorbing states and conservation of the number of particles [4–8].

Recently, Basu *et al.* showed in one dimension that the known models in the Manna class, i.e., the discrete and continuous conserved Manna models, yielded critical exponents similar to the DP values when generated from the initial states prepared in a particular way [9]. In the stochastic Manna model (hereafter called the Manna model), which is identical to the discrete conserved Manna model in Ref. [9], each lattice site is occupied by multiple particles; the sites occupied by two or more particles are considered to be active sites, and empty and singly occupied sites are considered to be inactive [10,11]. Starting from an initial state, the dynamics proceeds with hopping of active particles; each of the particles on randomly selected active sites hops to one of the neighboring sites. Two different types of updates, parallel and sequential updates, can be employed. In the parallel update, all active sites are updated at the same time with an increment of evolution time  $\Delta t = 1$ , whereas in the sequential update, randomly selected active sites are updated, each with an increment of  $\Delta t = 1/N_a(t)$ , with  $N_a(t)$  being the number of active sites at time  $t$ . There is no particle creation or annihilation during the dynamics and thus the number of particles is conserved.

Before the work of Basu *et al.* [9], all studies employed a random initial distribution of particles, i.e., random initial states [12]. The main concern in the previous study was that the random initial states yielded an inhomogeneous distribution of inactive singly occupied particles [9]. Such background particles may become active at a later time as dynamics proceeds and contribute to the critical behavior.

The inhomogeneous background field was claimed to cause an anomalous decay of active-site densities near and at the critical point, i.e., the active-site density decreased, reached a minimum, and then increased before saturation to a steady-state density. The undershooting of active-site densities caused a failure of scaling and made accurate estimation of the critical exponents difficult. Following an idea introduced earlier for the pair-contact process [13], Basu *et al.* prepared the natural initial states as follows. Starting from a random distribution of particles, let the simulation run until the steady state is achieved; from there, all particles are allowed to take a random-walk step to the nearest-neighbor sites. The configuration obtained in this way is called the “natural” initial state. They showed that the natural initial states eliminated such undershooting and that all models known to belong to the Manna class yielded the critical exponents similar to the DP values [9]. Based on the numerical analysis, they claimed that an independent Manna class did not exist and that all models in the Manna class were expected to show the DP critical behavior after a long time. On the other hand, in two dimensions, the critical behavior of the Manna model was found to be different from that of the DP class even when the dynamics proceeded from the natural initial states [14].

In this Rapid Communication, the Manna model was studied on a one-dimensional (1D) chain and on a diluted strip of  $L_x \times L_y$  lattice sites with  $L_x \gg L_y$ . Attention was paid particularly on whether or not the critical behavior was different from the DP critical behavior. On a 1D chain, the critical density was found to be slightly smaller and, accordingly, the order-parameter exponent was different from that of the earlier work [9]. The influence of quenched disorder was also found to be distinct from that of a prototype model in the DP class.

Starting from an initial distribution of particles of density  $\rho$ , the active-site density  $\rho_a(t)$  decays exponentially in time for  $\rho < \rho_c$ , saturates to a steady-state density  $\rho_{\text{sat}}$  for  $\rho > \rho_c$ , and decreases following the power law  $\rho_a(t) \sim t^{-\alpha}$  at the critical density  $\rho_c$ . A set of critical exponents is defined as in equilibrium critical phenomena by the order parameter  $\rho_{\text{sat}}(\epsilon) \sim \epsilon^\beta$ , the correlation length  $\xi \sim \epsilon^{-\nu_\perp}$ , and the correlation time  $\tau \sim \epsilon^{-\nu_\parallel} \sim \xi^z$  in the vicinity of criticality, where

$\epsilon = |\rho - \rho_c|$  is the distance from criticality and  $z = \nu_{\parallel}/\nu_{\perp}$  is the dynamic exponent. When  $\rho$  is slightly different from  $\rho_c$  for a system of size  $L$ ,  $\rho_a$  can be written as

$$\rho_a(t, \epsilon, L) = t^{-\alpha} \mathcal{F}(t\epsilon^{\nu_{\parallel}}, t/L^z). \quad (1)$$

In the  $t \rightarrow \infty$  limit on an infinite system, since  $\rho_a(\infty, \epsilon, \infty) = \rho_{\text{sat}}(\epsilon) \sim \epsilon^{\beta}$  as  $\rho \rightarrow \rho_{c+}$ , the relation  $\beta = \nu_{\parallel}\alpha$  is obtained. On the other hand, at criticality on a system of size  $L$ ,  $\rho_a(\infty, 0, L) = \rho_{\text{sat}}(L) \sim L^{-\beta/\nu_{\perp}}$  in the steady state. The universality classes are classified from the values of the critical exponents.

The stochastic Manna model is a simple model, but investigation of its critical behavior on a 1D chain is nontrivial, mainly because of the extremely slow decay of active-site densities. Basu *et al.* [9] calculated  $\rho_a(t)$  using the *parallel* update starting from the natural initial states and determined, from the power-law behavior of  $\rho_a(t)$ ,  $\rho_c = 0.89236(3)$ , which is slightly larger than the known value  $\rho_c = 0.89199(5)$  by Lübeck and Heger using the random initial states [12,15]. It is, however, believed that the critical density should be the same irrespective of the initial states because the data for  $\rho_{\text{sat}}(L)$  and  $\rho_{\text{sat}}(\epsilon)$  remain the same for both initial states and, accordingly, the power-law behaviors of both should hold equally for different initial states.

Since an accurate value of  $\rho_c$  is particularly important to estimate the critical exponents, extensive simulations were carried out using the natural initial states. The *sequential* update was employed because it turned out to be faster than the parallel update. For sufficiently large systems near and at  $\rho_c$ , the system never reached the steady state within an attainable evolution time and, accordingly, the natural initial states could not be prepared from the steady-state configurations. To see how the homogenization was achieved, the cumulative sums  $S_j = \sum_{i=1}^j n_i - (N/L)j$  defined in Ref. [9] were calculated for  $\rho = 0.89216$  and  $0.897$ , both on a system of size  $L = 10^5$ , and plotted in Fig. 1; from the figure, it is clear that the initial density fluctuations are leveled out after  $t = 10^8$  for both densities. (Note that homogenization is achieved one order faster than that in Ref. [9], presumably due to the different update rule.) Considering that the steady state was not reached at  $t = 10^8$  for  $\rho = 0.89216$ , it appeared that the initial memory

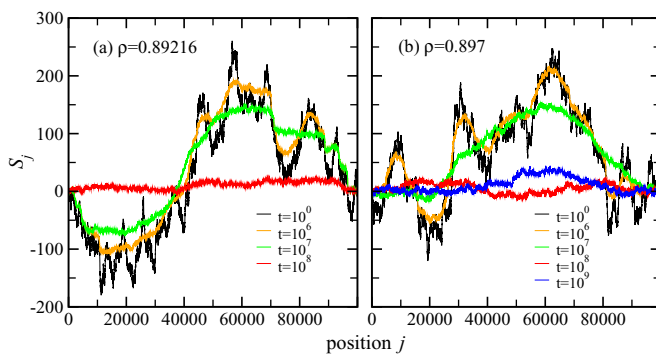


FIG. 1. (Color online) Plot of the cumulative particle density for a random initial state captured at different simulation times. (a) is for  $\rho = 0.89216$  and (b) is for  $\rho = 0.897$ . Data from the most fluctuating set to the least fluctuating set are for  $t = 1$  (black),  $10^6$  (orange),  $10^7$  (green),  $10^8$  (red), and  $10^9$  (blue) time steps.

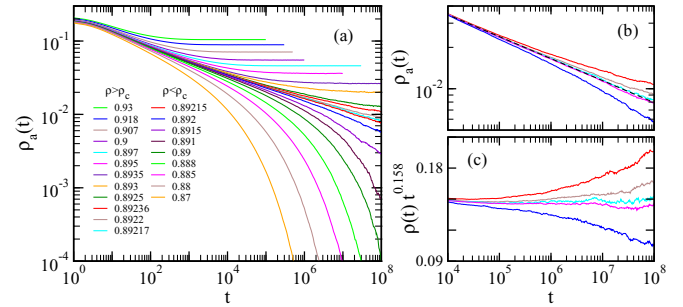


FIG. 2. (Color online) (a) Data of  $\rho_a(t)$  for selected particle densities in the 1D Manna model. (b) The selected data between the two known values of  $\rho_c$  on a larger scale. (c) The scaled data  $\rho_a(t)t^{\alpha}$  as a function of time. The numbers on the legend in (a) are the particle densities for the data in the same order from top to bottom.

of density fluctuation was lost after a long time regardless of whether or not the steady state was achieved. The natural initial states were thus prepared after relaxing the system up to  $10^9$  time steps (one order higher  $t$  for safety) for the densities close to and at  $\rho_c$ .

The data for  $\rho_a(t)$  were calculated for selected particle densities on a system of size  $L = 10^6$ , and the results were plotted in Fig. 2: (a) the raw data, (b) the data for five selected densities on a larger scale, and (c) the scaled data  $\rho_a(t)t^{\alpha}$  as a function of  $t$ . The data for  $\rho = 0.8920$  veer down and those of  $\rho = 0.89236$  veer up, suggesting that none of the known values is the true  $\rho_c$ . The asymptotic power law appeared to hold in the region  $10^4 \leq t \leq 10^8$  for  $\rho$  between  $0.89215$  and  $0.89217$ . Therefore,  $\rho_c = 0.89216(3)$  was obtained with  $\alpha \simeq 0.158$ . [Note that Basu *et al.* obtained  $\rho_c$  from the power law of  $\rho_a(t)$  up to  $10^7$  time steps.]

The steady-state densities for  $\rho > \rho_c$  were calculated from the data in Fig. 2(a) and also from simulations on a system of size  $L = 2^{18}$  for comparison with the data in Ref. [9]. It should be noted that the size of system  $L = 10^6$  is much larger than those of Refs. [9,12],  $L = 2^{18} = 262144$  and  $L = 2^{13}$ , respectively. Figure 3 shows  $\rho_{\text{sat}}(\epsilon)$ ; the lower set is for  $\rho_c =$

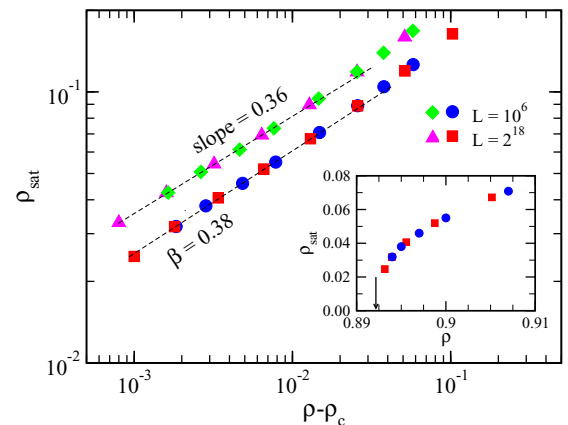


FIG. 3. (Color online) Data of  $\rho_{\text{sat}}(\epsilon)$  in the 1D Manna model. The upper set is for  $\rho_c = 0.89236$  which is shifted upward by multiplying 1.5 and the lower set for  $\rho_c = 0.89216$ . The inset shows the raw data, with the arrow marking  $\rho_c$ .

0.892 16 and the upper set shifted upward is for  $\rho_c = 0.892 36$ . Data for  $\epsilon \leq 0.02$  ( $\rho_c < \rho < 0.91$ ) in the lower set yielded the power-law behavior, with the power of  $\beta = 0.380(5)$  (lower dashed line), which is consistent with the value  $\beta = 0.382(19)$  by Lübeck [15] but is off from the DP value of  $\beta_{\text{DP}} = 0.2763$ . A slight deviation of the leftmost data for  $L = 2^{18}$  from the power-law fit appears to be due to the finite-size effect.

Basu *et al.* found that a log-log plot of  $\rho_{\text{sat}}(\epsilon)$  against  $\epsilon$  with a larger value of  $\rho_c$  yielded a curvature for an entire region of  $\epsilon$ . Plotting the effective exponent against  $\epsilon^{0.45}$ , they obtained a value of  $\beta$  close to the DP value. However, because  $\epsilon > 0.02$  is far from the critical point and might be out of the scaling region, it is not clear whether the correction-to-scaling analysis by taking the trend of the data in such a region into account is valid. In our data, however, the significant upward curvature was not observed for  $\epsilon \leq 0.02$  as  $\rho \rightarrow \rho_{c+}$ , as was seen in Fig. 2; thus the correction fit was unnecessary. It was also noticed that special attention should be paid to unbiased sampling when collecting data from the nodes of the Message Passing Interface (MPI) system running in parallel, particularly close to  $\rho_c$ . Since computing time varies over realizations due to fluctuations of  $\rho_a(t)$ , those of smaller  $\rho_a(t)$  apparently take less CPU time. As a result, it was found that, when collecting data in a series,  $\rho_a(t)$  in the large  $t$  region ( $t \geq 10^4$ ) increased gradually as the number of realizations increased, because realizations of larger  $\rho_a(t)$  were collected later. Therefore, in order not to lose the realizations of long computing time, simulations should not be stopped until the accumulated data yield stationary results. If it is stopped before then, the collected data should be discarded for the unbiased sampling. (Note that the data at  $\rho_c$  took approximately 2000 h with 40 cores of Pentium-3.2 GHz running in parallel.)

In order to verify the estimates of  $\rho_c$ ,  $\alpha$ , and  $\beta$ , the off-critical scaling was examined. Figure 4 shows the off-critical scaling function in Eq. (1),  $\rho_a t^\alpha = \mathcal{F}(t\epsilon^{\nu_{\parallel}}, \infty)$ , scaled using  $\rho_c = 0.892 16$ ,  $\alpha = 0.158$ , and  $\nu_{\parallel} = \beta/\alpha = 2.405$  [Fig. 4(a)] and  $\rho_c = 0.892 36$ ,  $\alpha = 0.159$ , and  $\nu_{\parallel} = 1.733$  (known DP values) [Fig. 4(b)] for the data within the scaling region in Fig. 3 ( $\epsilon \leq 0.02$ ). In Fig. 4(a), data in the supercritical region fall onto a single curve, i.e., scaling holds, whereas in the subcritical region data collapsing is a bit poor. In Fig. 4(b),

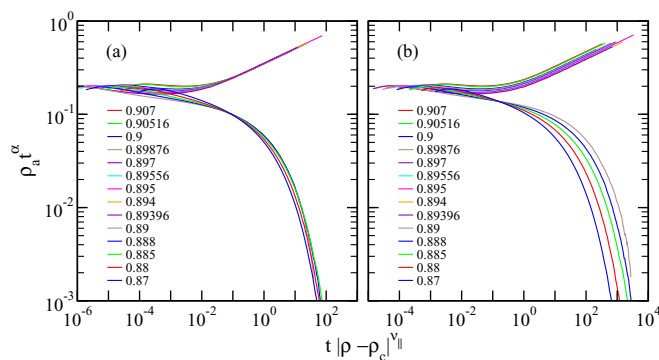


FIG. 4. (Color online) Off-critical scaling function of  $\rho_a(t)$  scaled with (a)  $\rho_c = 0.892 16$ ,  $\alpha = 0.1581$ , and  $\nu_{\parallel} = 2.404$  and (b)  $\rho_c = 0.892 36$ ,  $\alpha = 0.159$ , and  $\nu_{\parallel} = 1.733$  (DP values). The numbers in the legends are the particle densities for the data in the same order.

on the other hand, the scaling fails in both regions. It is clear that the values used in Fig. 4(a) are more reliable. Poor scaling in the subcritical region in Fig. 4(a) might be attributed to an inhomogeneous distribution of background particles. In the subcritical region, the system fell into an absorbing state before homogenization was achieved. Nonetheless, eliminating data for  $\rho = 0.87$  and  $0.88$ , scaling held fairly well; the scaling region is thus relatively narrow for  $\rho < \rho_c$ . (Note that the system for these  $\rho$  values did not survive up to the time required for homogenization.)

The distinct behavior of the Manna model from that of the contact process (CP) [16] was also observed on the responses to the quenched disorder added in the system. The CP is defined as that particles either spread ( $A \rightarrow AA$ ) with a rate  $\lambda$  or become extinct ( $A \rightarrow 0$ ) with a rate  $\mu$  (usually set  $\mu = 1$ ). For  $\lambda > \lambda_c$ , the system remains in an active phase, whereas for  $\lambda < \lambda_c$ , the system falls into a single absorbing state of a vacuum. The influence of quenched disorder on the CP was first studied by Moreira and Dickman [17] and it has been recently studied more extensively in 1D [18,19]. It is now widely known that the particle density  $\rho_a(t)$  exhibits nonuniversal power-law behavior in the Griffith phase of  $\lambda_c^0 < \lambda < \lambda_c$ , where  $\lambda_c^0$  and  $\lambda_c$  are the critical spreading rates on a pure system and on a disordered system, respectively. Such a nonuniversal power-law decrease on a disordered lattice is typical for models in the DP class, such as CP [17–19] and cellular automata [20].

The quenched disorder in the 1D CP is defined by a binary probability distribution  $P(\lambda(\mathbf{r})) = (1 - p)\delta(\lambda(\mathbf{r}) - \lambda) + p\delta(\lambda(\mathbf{r}) - c\lambda)$ , where  $p$  and  $c$  represent, respectively, the concentration of impurity sites and the relative strength of the impurities. In this expression, the randomly selected  $pL$  sites are assigned as impurity sites and, in each impurity site, the spreading rate is suppressed by a factor  $c$  ( $< 1$ ). For the Manna model, however, similar disorder cannot be set because of conservation of the number of particles. In two and higher dimensions, on the other hand, the diluted sites are assumed to be disordered sites [17,21]. Therefore, an infinite percolation cluster can be considered as the disordered lattice. On a 1D chain, since any diluted site fragments the system into smaller clusters, a diluted infinite cluster cannot be set. On the other hand, the sites on a  $L_x \times L_y$  ( $L_x \gg L_y$ ) strip can be diluted without fragmenting the system, thus enabling one to study the influence of disorder in one dimension.

The active site densities were compared for the two models on a strip of  $10^5 \times 20$  sites, with  $p = 0.2$ . The periodic boundaries were set along the  $x$  direction and the free boundaries along the  $y$  direction. Figure 5 shows  $\rho_a(t)$  of the CP on an undiluted strip. The data yielded a larger local slope in the early time, which is a transient 2D behavior and, for  $t > 10^2$ ,  $\rho_a(t)$  exhibited the 1D critical behavior. It appears that  $\lambda_c \simeq 1.709 41$ , with  $\alpha \simeq 0.16$  (inset), which is close to the known DP value in one dimension. The steady-state densities calculated from the figure also yielded a power-law decrease, when plotted against  $\lambda - \lambda_c$ , with the power  $\beta \simeq 0.28$  (not shown), which is again close to the DP value.

Figure 6(a) shows  $\rho_a(t)$  for the CP on a strip diluted with  $p = 0.2$  for selected values of  $\lambda > \lambda_c^0$ . The data yield a nonuniversal power-law decrease, with the power depending on the value of  $\lambda$ , suggesting the presence of the Griffith

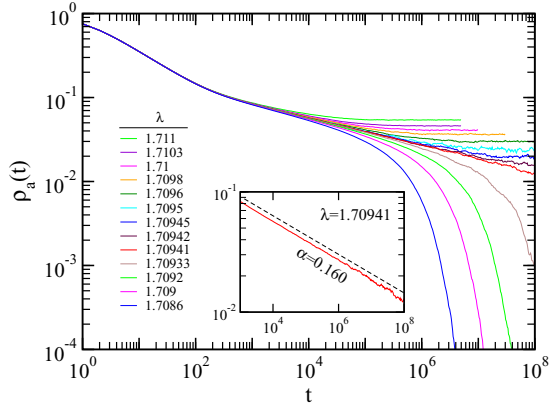


FIG. 5. (Color online) Data of  $\rho_a(t)$  for the CP on a strip of  $10^5 \times 20$  lattice sites. The inset shows the data that yield the best power law, with  $\alpha \simeq 0.16$ . The numbers in the legend are the spreading rates for the data in the same order.

phase. However, for the Manna model, the selected data for  $\rho > 0.7483$  saturated to steady-state densities and those for  $\rho < 0.7483$  decayed exponentially, rather than following nonuniversal power laws, as can be seen in Fig. 6(b). (It appears that  $0.704 < \rho_c < 0.705$  for the Manna model on a clean strip.) The plot clearly shows a behavior different from that of the CP. If one naively estimates  $\beta$  from the data in Fig. 6 assuming  $\rho_c$  as a parameter, it would be  $\beta \approx 0.35$ , which is close to the 1D value. One may, however, raise a possible concern that the two models exhibit the same DP critical behavior on a clean lattice but they may respond differently to the disorder. We cannot rule out such a possibility; however, using the language of the renormalization group theory, the clean fixed point of the CP is unstable whereas that of the Manna model appears to be stable; therefore, the two models should be distinguished. This is in a similar situation to the 2D case, in which disorder was irrelevant as long as the disorder concentration was less than the critical concentration [22]. In the recent study in 2D, the two known models in the Manna class were found to yield consistent exponent values within an error of 1% but they were 7%–12% off from the DP values [23]. It is also worth

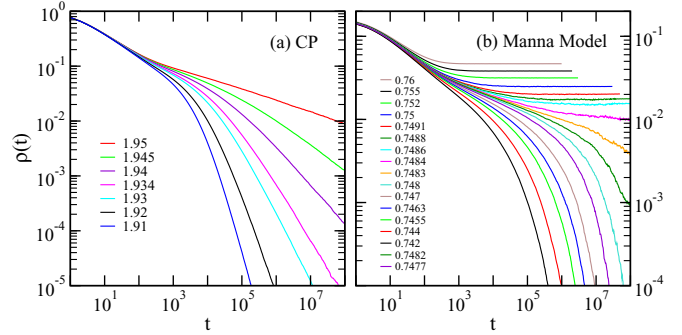


FIG. 6. (Color online) Data of  $\rho_a(t)$  for the (a) CP and (b) Manna model, both on a strip of  $10^5 \times 20$  sites with 20% of the sites diluted. The numbers on the legend in (a) are the spreading rates and in (b) the particle densities for the data in the same order.

noting that, according to the Harris criterion [24], the clean fixed point is unstable if  $d\nu_{\perp} < 2$ . The inequality holds for the both CP and Manna model in both dimensions; however, the Harris criterion established for equilibrium magnetic systems is now known to be invalid for nonequilibrium APTs [14,22,25].

In summary, the critical behavior of APTs was studied for the 1D Manna model with the natural initial states, using the sequential update rule. On a chain, the critical density was found to be slightly smaller than that of the earlier work and, with the estimate, the order-parameter exponent was considerably larger than the DP value. The influence of quenched disorder was also investigated on a strip of  $10^5 \times 20$  sites, with 20% of the sites diluted. For the CP, the active-particle density exhibited a nonuniversal power-law decrease in the region  $\lambda_c^0 < \lambda < \lambda_c$ , whereas for the Manna model the active-site density yielded a standard critical behavior. The results on a chain and on a diluted strip both suggested that the Manna model should be distinguished from the models in the DP universality class.

This work was supported by the Korea Research Foundation Grant (2011-0010924).

- [1] For a review, see, e.g., J. Marro and R. Dickman, *Nonequilibrium Phase Transitions in Lattice Models* (Cambridge University Press, Cambridge, UK, 1999); H. Hinrichsen, *Adv. Phys.* **49**, 815 (2000).
- [2] H. K. Jansen, *Z. Phys. B: Condens. Matter* **42**, 151 (1981).
- [3] P. Grassberger, *Z. Phys. B: Condens. Matter* **47**, 365 (1982).
- [4] H. Takayasu and A. Y. Tretyakov, *Phys. Rev. Lett.* **68**, 3060 (1992).
- [5] I. Jensen, *Phys. Rev. E* **50**, 3623 (1994).
- [6] S. Kwon and H. Park, *Phys. Rev. E* **52**, 5955 (1995).
- [7] J. Cardy and U. C. Täuber, *Phys. Rev. Lett.* **77**, 4780 (1996).
- [8] M. Rossi, R. Pastor-Satorras, and A. Vespignani, *Phys. Rev. Lett.* **85**, 1803 (2000).
- [9] M. Basu, U. Basu, S. Bondyopadhyay, P. K. Mohanty, and H. Hinrichsen, *Phys. Rev. Lett.* **109**, 015702 (2012).
- [10] S. S. Manna, *J. Phys. A* **24**, L363 (1991).
- [11] A. Vespignani, R. Dickman, M. A. Munõz, and S. Zapperi, *Phys. Rev. E* **62**, 4564 (2000).
- [12] S. Lübeck and P. C. Heger, *Phys. Rev. E* **68**, 056102 (2003).
- [13] I. Jensen and R. Dickman, *Phys. Rev. E* **48**, 1710 (1993).
- [14] S. B. Lee, *Phys. Rev. Lett.* **110**, 159601 (2013).
- [15] S. Lübeck, *Int. J. Mod. Phys. B* **18**, 3977 (2004).
- [16] T. E. Harris, *Ann. Probab.* **2**, 969 (1974).
- [17] A. G. Moreira and R. Dickman, *Phys. Rev. E* **54**, R3090 (1996); R. Dickman and A. G. Moreira, *ibid.* **57**, 1263 (1998).
- [18] J. Hooyberghs, F. Iglói, and C. Vanderzande, *Phys. Rev. Lett.* **90**, 100601 (2003); *Phys. Rev. E* **69**, 066140 (2004).

- [19] T. Vojta and M. Dickison, *Phys. Rev. E* **72**, 036126 (2005).
- [20] A. J. Noest, *Phys. Rev. Lett.* **57**, 90 (1986).
- [21] T. Vojta, A. Farquhar, and J. Mast, *Phys. Rev. E* **79**, 011111 (2009).
- [22] S. B. Lee, *Phys. Rev. E* **84**, 041123 (2011).
- [23] S. B. Lee, *Phys. Rev. E* **89**, 062133 (2014).
- [24] A. B. Harris, *J. Phys. C* **7**, 1671 (1974).
- [25] G. Ódor and N. Menyhárd, *Phys. Rev. E* **73**, 036130 (2006).